

# Aperiodic stochastic resonant data storage on directed small-world networks

Fabing Duan<sup>a</sup> and Derek Abbott<sup>b</sup>

<sup>a</sup>Institute of Complexity Science, Qingdao University, Qingdao 266071, PR China;

<sup>b</sup>Centre for Biomedical Engineering (CBME) and School of Electrical & Electronic Engineering, The University of Adelaide, Adelaide, SA 5005, Australia

## ABSTRACT

We study aperiodic stochastic resonant data storage in an extended system evolving on directed small-world networks. Each node of the network represents a dynamical bistable system, and nodes are randomly connected by the directed shortcuts with a rewiring probability. The constructive role of the internal noise and the random connectivity is characterized by the bit error rate and demonstrated in numerical simulations. Random internal noise in each node enhances the survival of a short-time length of binary signal via aperiodic stochastic resonance. Interestingly, random connectivity further improves the propagation time of binary information through the small-world architecture.

**Keywords:** Bistable system, Aperiodic stochastic resonance, Internal noise, Random connectivity, Directed small-world network

## 1. INTRODUCTION

Currently, it is well known that noise in nonlinear systems has a profound effect on their dynamics. Noise-enhanced phenomena such as stochastic resonance (SR) and coherence resonance have fueled studies across diverse fields of research over decades.<sup>1,2</sup> Originally, the majority of noise-enhanced phenomena dealt with the dynamics of an individual nonlinear system. The prototype SR model is an overdamped bistable system, which was used to describe the earth's climatic change.<sup>3</sup> Later, non-bistable systems, such as the excitable system<sup>4</sup> and the threshold detector,<sup>5</sup> have been introduced to pave the way for applications of SR in neurophysiology. Meanwhile, researchers considered the influence of structure on SR,<sup>6-15</sup> because structure always affects function.<sup>16,17</sup> The regular structure of nonlinear systems was first introduced in the study of globally coupled or uncoupled bistable systems.<sup>6,7</sup> Some interesting studies are worthy of notice, e.g. array enhanced SR in a chain of identical resonators,<sup>8</sup> SR without tuning<sup>9</sup> and suprathreshold SR in a parallel array of uncoupled nonlinear systems,<sup>10</sup> spatiotemporal SR in excitable media,<sup>11</sup> stochastic resonant memory storage device in a ring,<sup>12</sup> and noise-enhanced memory in neural networks.<sup>13-15</sup> The common feature of these studies is that the structure of extended systems is regular.<sup>6-15</sup>

Although regular network is a useful idealization, many real networks exhibit various network topologies. One of the most interesting network structures is a small-world model between regular and random networks studied by Watts and Strogatz.<sup>16,18</sup> If the networks are directed and exhibit links that are definitely asymmetric, i.e. directed small-world network.<sup>21</sup> Researchers found that dynamical systems coupled in the small-world structure display enhanced signal propagation speed, synchronizability and computational power, as compared with regular lattices of the same size.<sup>16-23</sup> It is worthy of noting that this kind of structure existed before the term of small-world was coined.<sup>16-18,24-26</sup> For example, small-world neuron connectivity in the cortex or other brain regions was observed to improve the function of neural networks.<sup>24-26</sup> Naturally, the focus of SR studies has also shifted from the regular structure of nonlinear extended systems towards more complex networks, especially small-world networks.<sup>27-34</sup> SR of a coupled array of bistable oscillators with small-world connectivity was first studied.<sup>27</sup> It is found that temporal SR and spatial synchronization of the oscillators can be considerably improved upon

---

Further author information: (Send correspondence to Dr. F. Duan)

E-mail: fabing1974@yahoo.com.cn (Dr. F. Duan);

E-mail: dabbott@eleceng.adelaide.edu.au (Prof. D. Abbott)

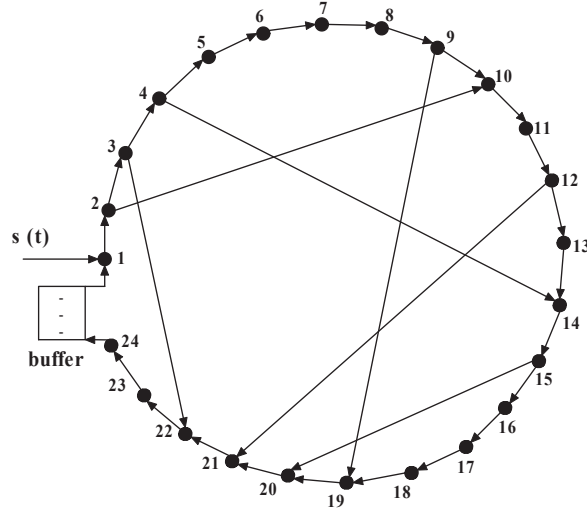


Figure 1. An example of a directed small-world network with  $N = 24$ ,  $\rho = 1/4$  and 6 shortcuts. Each node represents a dynamical nonlinear system, and arrows mean the direction of signal propagation. Here,  $s(t)$  is the binary pulse-amplitude modulated signal and survives for a time length  $T$ . The buffer stores the output of the 24th node for a time length larger than  $T$ , and, after each loop of network evolution, pours the stored data into the first node as its input.

increasing the order of randomness of the network due to the long-range coupling.<sup>27</sup> The SR behavior of an Ising model was researched in the presence of temporally oscillating external magnetic fields.<sup>30</sup> Since the small-world network is confirmed in neuroscience to a great extent,<sup>24–26</sup> the FitzHugh-Nagumo<sup>28,29,31,34</sup> and Hodgkin-Huxley<sup>33</sup> neuron models were also extensively investigated. The impact of subthreshold pacemaker activity on the temporal dynamics of noisy excitable small-world networks was studied with a view to medical applications.<sup>32</sup> These studies show that noise plays a positive role in network dynamics, and the small-world structure also presents a crucial role in network evolution and function.

Thus, we recognize that noise and complex structure are both constructive ingredients from the perspective of nonlinear dynamical systems. In this paper, we will study aperiodic stochastic resonant data storage in bistable systems evolving on a directed small-world network. It has been shown that the ring of bistable systems as a short-term memory device in which the stored sinusoidal wave is sustained by internal noise.<sup>12</sup> The long-term noise-induced memory was described in one-dimensional coupled excitable systems.<sup>15</sup> In our work, we mainly explore the roles of both the small-world topological network of dynamical systems and internal noise in the short-term binary modulated signal storage. We first introduce how the directed links grow into the small-world networks, and then drive the network with a short-term binary signal by varying other parameters. The performance of network is measured by the bit error rate (BER) and the simulation results demonstrate the positive roles of both the internal noise in network and the random connectivity of network.

## 2. DIRECTED SMALL-WORLD MODEL OF BISTABLE SYSTEMS

We consider the topology of a directed small-world network shown in Fig. 1, composed of  $N = 24$  vertices with bonds between nearest neighbors and periodic boundary conditions (the lattice is a ring initially). There are  $N$  link edges and the links between vertices are directed by arrows.<sup>19,21</sup> Then, this original lattice is rewired at random with rewiring probability  $\rho$ , so that there are  $\rho N$  shortcuts on average. Note that the number of both vertices and original edges remain unchanged.<sup>19</sup> In this model, the average coordination number  $z$  is  $z = 2(1 + \rho)$ . This model is equivalent to the Watts-Strogatz model for small  $\rho$ , whilst being better behaved<sup>19</sup> when  $\rho$  becomes comparable to 1. An example of this model is shown in Fig. 1.

Each node represents a bistable oscillator, and their dynamics are governed by

$$\begin{aligned}\tau_a \frac{dx_1(t)}{dt} &= x_1(t) - \frac{x_1^3(t)}{X_b^2} + s(t) + \epsilon x_N(t-T) + \eta_1(t), \\ \tau_a \frac{dx_i(t)}{dt} &= x_i(t) - \frac{x_i^3(t)}{X_b^2} + \epsilon x_{i-1}(t) + \sum_{j < i-1} \epsilon_{ij} x_j(t) + \eta_i(t), \quad i, j = 2, 3, \dots, N,\end{aligned}\quad (1)$$

where the real tunable array parameters  $\tau_a$  and  $X_b$  are in the dimensions of time and amplitude, respectively.<sup>35</sup> The first bistable oscillator is subject to a baseband binary pulse amplitude modulation signal  $s(t)$  lasting the time length  $T$ , where  $s(t) = A$  corresponds to digit 1 and  $s(t) = -A$  to digit 0 within a time interval of  $t_p$ . Here,  $A$  is the pulse amplitude and  $t_p$  is the pulse duration. Thus, there are  $T/t_p$  bits of the information content in  $s(t)$ . At the same time, zero-mean Gaussian white noise  $\eta_i(t)$ , together with and independent of  $s(t)$ , is applied to each oscillator of the small-world model. The  $N$  internal noise terms  $\eta_i(t)$  are mutually independent<sup>35</sup> and have autocorrelation  $\langle \eta_i(t)\eta_i(0) \rangle = 2D\delta(t)$  with a same noise intensity  $D$ . The coupling strength of the original ring is  $\epsilon$  and  $\epsilon > 0$ , while the the coupling  $\epsilon_{ij}$  between two oscillators are determined by the coupling pattern of the small-world model. If two oscillators are coupled and  $\epsilon_{ij} = \epsilon$ , otherwise  $\epsilon_{ij} = 0$ . The link of signal propagation is directed (asymmetric), and the index  $j < i - 1$  for  $i, j = 2, 3, \dots, N$  in Eq. 1. Note that the input signal  $s(t)$  only exists for a time length of  $T$ , and the evolution of network will be sustained by the internal oscillations  $x_i(t)$  after  $t > T$ .

Rescale the variables according to

$$x_i(t)/X_b \rightarrow x_i(t), A/X_b \rightarrow A, D/(\tau_a X_b^2) \rightarrow D, t/\tau_a \rightarrow t, T/\tau_a \rightarrow T, t_p/\tau_a \rightarrow t_p, \epsilon \rightarrow \epsilon, \epsilon_{ij} \rightarrow \epsilon_{ij}, \quad (2)$$

where each arrow points to a dimensionless variable. Equation (1) is then recast in a dimensionless form as

$$\begin{aligned}\frac{dx_1(t)}{dt} &= x_1(t) - x_1^3(t) + s(t) + \epsilon x_N(t-T) + \eta_1(t), \\ \frac{dx_i(t)}{dt} &= x_i(t) - x_i^3(t) + \epsilon x_{i-1}(t) + \sum_{j < i-1} \epsilon_{ij} x_j(t) + \eta_i(t), \quad i, j = 2, 3, \dots, N.\end{aligned}\quad (3)$$

Here,  $s(t)$  is a subthreshold input as the dimensionless amplitude  $A < A_c = 2/\sqrt{27} \approx 0.385$ , otherwise a suprathreshold signal.<sup>1, 35</sup> In this paper, we numerically integrate the stochastic differential equation<sup>36</sup> of Eq. (3) using the Euler-Maruyama discretization method with a small sampling time step  $\Delta t \ll t_p$ . The continuous noise background in the input power spectral density, is specified by the variance  $\sigma^2 = 2D/\Delta t$ . Here, the rms amplitude of internal noise  $\eta_i(t)$  is  $\sigma$ .

After the time span of  $nT$  ( $n = 1, 2, \dots$ ), we sample the output  $x_N$  of the last node at equispaced times  $t_j = (n-1)T + jt_p$  for  $j = 1, 2, \dots$ . Then, each  $x_N(t_j)$  is compared to the decision threshold  $\ell = 0$  for decoding the digits 0 or 1: If  $x_N(t_j) > 0$ , the decoded digit is one, otherwise it is zero.<sup>36</sup> An information measure, the BER, will be used to quantify the performance of this small-world network for data storage. We assume that the input binary digits occur with equal probabilities, i.e.,  $P(0) = P(1) = 1/2$ , and are statistically independent.  $P(0)$  and  $P(1)$  represent the probabilities of digits 0 and 1 at the input, respectively. In the presence of noise,  $P(0|1)$  is the probability of error for the decoded output to be 0 when the input digit is 1, and conversely for  $P(1|0)$ . Thus, the total probability of error  $P_e$  reads

$$P_e = P(0)P(1|0) + P(1)P(0|1). \quad (4)$$

Since each erroneous output digit will lose one bit of information,  $P_e$  is also called the BER. However, the time delay of the network output is considerable large, and the input-output synchronization loses. Here, we compare the input binary information with the decoded digits by interleaved subscript. In the following simulation experiments of Sec. 3, the minimal value of  $P_e$  yielded by interleaving comparison is recorded as the final simulation result.

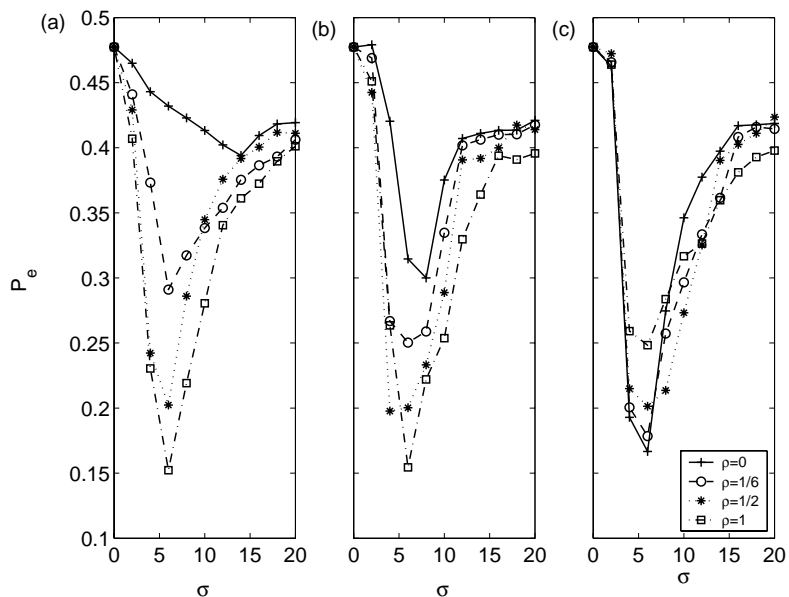


Figure 2. The BER  $P_e$  as a function of the internal noise rms amplitude  $\sigma$  for the signal amplitude  $A = 0.2$  and several probabilities  $\rho$  (see legends). The coupling strength is (a)  $\epsilon = 0.9$ , (b)  $\epsilon = 1.05$  and (c)  $\epsilon = 1.5$ .

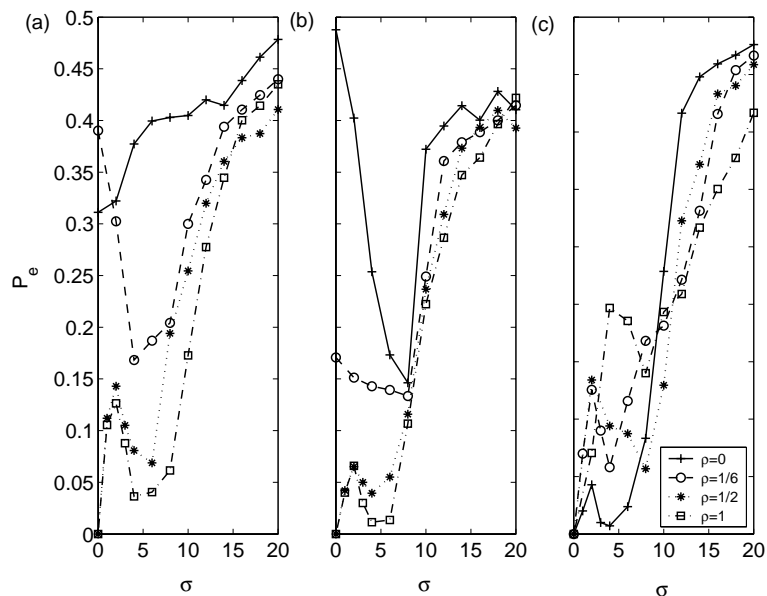


Figure 3. The BER  $P_e$  as a function of the internal noise rms amplitude  $\sigma$  for the signal amplitude  $A = 0.4$  and several probabilities  $\rho$  (see legends). The coupling strength is (a)  $\epsilon = 0.9$ , (b)  $\epsilon = 1.05$  and (c)  $\epsilon = 1.5$ .

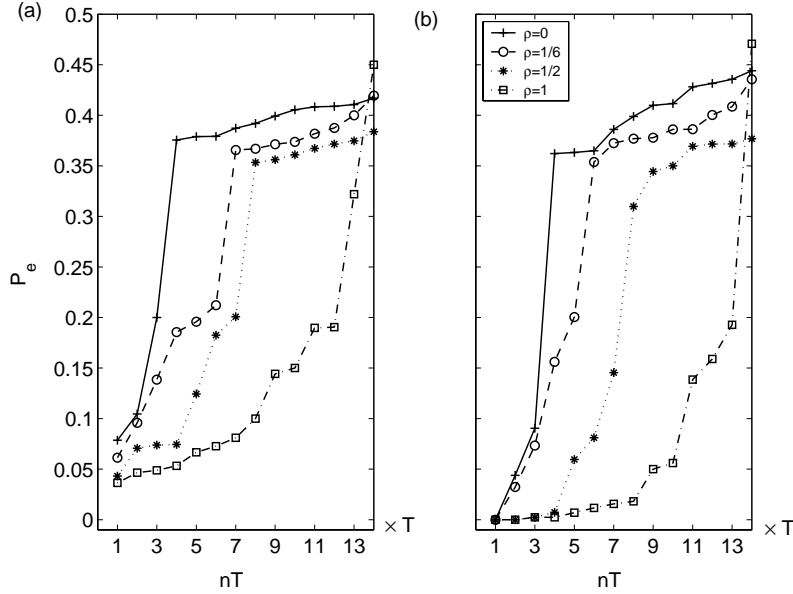


Figure 4. The BER  $P_e$  as a function of the evolution time of  $nT$  for the signal amplitude (a)  $A = 0.35$  (subthreshold) and (b)  $A = 1.0$  (suprathreshold). Here, the internal noise rms amplitude  $\sigma = 6$ , several probabilities  $\rho$  are indicated in legends and the coupling strength is  $\epsilon = 1.05$ .

### 3. EXPERIMENTAL RESULTS

In numerical simulations, we generate ten different directed small-world networks for a given rewiring probability  $\rho$ , and each kind of network represents a specific connected pattern with a same rewiring probability.<sup>19,27</sup> The average results will be plotted for the cases considered in this paper.<sup>19,27</sup> We simulate the network model of Eq. 3 in these conditions: (i) For a given evolution time of  $3T$ , we analyze the effect of aperiodic SR for different values of the amplitude  $A$ , the coupling strength  $\epsilon$  and the rewiring probability  $\rho$ ; (ii) Some sets of parameters  $A$ ,  $\epsilon$  and  $\rho$  are selected, and the performance of networks will be depicted as a function of the evolution time of  $nT$  ( $n = 1, 2, \dots$ ) in a given internal noisy environment.

Figure 2 shows the BER of  $P_e$  as a function of internal noise rms amplitude  $\sigma$  for  $A = 0.2$  for various values of  $\rho$  and  $\epsilon$ . The total evolution time of network is three loops of  $3T$ . Here,  $s(t)$  is a subthreshold input signal with  $t_p = 20$ , and lasts in a time length of  $T = 900$ . The conventional aperiodic SR is obvious in Fig. 2. We see that the aperiodic SR effect can be enhanced by the increase of the rewiring probability  $\rho$  for  $\epsilon = 0.9 < 1$  and  $\epsilon = 1.05 > 1$ , as shown in Fig. 2 (a) and (b), respectively. The best performance of  $P_e$  occurs at  $\rho = 1$  (square) and  $\sigma = 6$ . However, if a strong coupling strength  $\epsilon = 1.5$ , increasing the random connection of  $\rho$  will weaken the aperiodic SR effect, as shown in Fig. 2 (c). The lowest  $P_e$  corresponds to the probability  $\rho = 0$  and the increase of randomly shortcuts will be useless for improving the BER. Thus, the positive role of the random connectivity of networks is close relative to the coupling strength  $\epsilon$ .

When we increase the input signal amplitude  $A$  to  $0.4$  ( $A > A_c$ ),  $s(t)$  is a slightly suprathreshold input. The performance of networks  $P_e$ , as a function of internal noise rms amplitude  $\sigma$ , is plotted in Fig. 3 for various values of  $\rho$  and  $\epsilon$ . We find that the aperiodic SR disappears for weak coupling strength  $\epsilon = 0.9$  and rewiring probability  $\rho = 0$ , as shown in Fig. 3 (a) (pluses). Upon increasing  $\epsilon$  and  $\rho$ , the conventional aperiodic SR and the residual aperiodic SR<sup>36</sup> will occur, as illustrated in Fig. 3 (a) and (b). The curve of residual aperiodic SR first starts from zero value of  $P_e$  as  $A > A_c$ , and then reaches to a relative higher value of  $P_e$  due to the injection of internal noise, and finally evolves as the curve of the conventional aperiodic SR effect.<sup>36</sup> This feature is more obvious for a large coupling strength  $\epsilon = 1.5$ , as shown in Fig. 3 (c). Also, Fig. 3 (c) indicates that the increase of the rewiring probability  $\rho$  degrades the effect of residual aperiodic SR, e.g.  $P_e$  of the network with  $\rho = 1$  as plotted in Fig. 3 (c) (squares). Other values of input signal amplitude  $A$  are also adopted in numerical simulations, such

as  $A = 0.35 < A_c$  (not shown here). The same results are obtained: For weak coupling coefficient ( $\epsilon = 0.9 < 1$ ) or slightly strong coefficient  $\epsilon = 1.05 > 1$ , the random connected shortcuts will enhance the performance of network. At an optimal regions of internal noise intensity, the higher  $\rho$  is, the lower  $P_e$  is calculated. However, increasing the rewiring probability  $\rho$  will be harmful for a strong coupling strength of  $\epsilon = 1.5$ .

For a given internal noise with rms amplitude of  $\sigma = 6$  and the coupling strength  $\epsilon = 1.05$ , Fig. 4 shows  $P_e$  versus the evolution time of  $nT$  for  $n = 1, 2, \dots$ . An input signal with subthreshold amplitude  $A = 0.35$  or suprathreshold one  $A = 1.0$ , as shown in Fig. 4 (a) and (b) respectively, is injected into the network, and the total evolution time is taken as  $14T$ . For each loop of the simulation, we record  $P_e$  for various rewiring probability  $\rho$ . It is seen that when the random connections of shortcuts are added gradually,  $P_e$  will be more lower even after many loops of network evolutions, e.g.  $P_e = 0.09$  at  $8T$  as shown in Fig. 4 (a) (squares). Thus, we can elicit that the increase of  $\rho$  will improve the informative data storage in a network with the coupling strength  $\epsilon = 1.05$  for both subthreshold and suprathreshold inputs.

The mechanism of noise-enhanced binary information storage is due to the SR effect, as shown in Figs. 2 and 3. For a subthreshold or slightly suprathreshold input, an optimal amount of internal noise will induce the inter-transition between bistable wells that correspond to digits 0 and 1. Too little or too much noise will cause the switching errors resulting in higher BERs. Furthermore, when the shortcut is added into the ring structure of the initial regular network, described by the rewiring connected probability  $\rho$ , the inter-transition switching errors can be deduced because of the reinforcement of the input amplitude of the connected nodes. Of course, if the internal noise is too strong and its the rms amplitude is larger than  $A$ , the addition of shortcuts to the network enlarge the switching errors induced by noise. Thus, the network with a higher  $\rho$  yields a larger  $P_e$  at the region of strong internal noise intensity, as plotted in Figs. 2 and 3. Similarly, if the coupling strength is strong enough, the random connection between nodes is also of no help, as shown in Fig. 2 (c). The benefit of the random connectivity of networks mainly depends on the coupling strength, while the constructive role of internal noise is involved in both the coupling strength and the signal amplitude.

#### 4. CONCLUSIONS

In this paper, we studied a directed small-world network model for storing a short-term binary information. Each node represents a bistable dynamical system buried in an internal noisy environment. Initially, a ring structure is operated and then some shortcuts are added to this regular network. The information stream is steered by the directional shortcuts, i.e. flowing in a directed small-world network. For various parameters of the signal amplitude, the coupling strength, and the rewiring connection probability, the numerical simulations show that the aperiodic SR occurs for subthreshold or slight suprathreshold input signals, and is also enhanced by the random connections between nodes. This point manifested in the simulation experiments considered in a fixed time length of three loops of network evolution. In a given moderate rms amplitude of internal noise, the survival feature of binary information was described the BER at each loop of network evolution for both subthreshold and suprathreshold inputs. The more shortcuts is added, the lower BER is obtained at an appropriate coupling strength. Finally, we argued that both random noise in each node and random connection between nodes of networks are of help in the information propagation in a directed small-world network in certain conditions considered in this paper. Future studies of such kind of networks connected with neuronal models will be of interest.

#### ACKNOWLEDGMENTS

This work is sponsored by NSFC (No. 60602040), Taishan Scholar CPSP of China. Funding from the Australian Research Council (ARC) is gratefully acknowledged.

#### REFERENCES

1. L. Gammaitoni, P. Hänggi, P. Jung, and F. Marchesoni, "Stochastic resonance," *Rev. Mod. Phys.* **70**, pp. 233-287 1998.
2. F. Sagués, J. M. Sancho, and J. García-Ojalvo, "Spatiotemporal order out of noise," *Rev. Mod. Phys.* **79**, pp. 829-882 2007.



3. R. Benzi, A. Sutera and A. Vulpiani, "The mechanism of stochastic resonance," *J. Phys. A: Math. Gen.* **14**, pp. L453-L457 1981.
4. A. Longtin, "Stochastic resonance in neuron models," *J. Stat. Phys.* **70**, pp. 309-327 1993.
5. P. Jung, "Threshold devices: fractal noise and neural talk," *Phys. Rev. E* **50**, pp. 2513-2522 1994.
6. P. Jung, U. Behn, E. Pantazelou, and F. Moss, "Collective response in globally coupled bistable systems," *Phys. Rev. A* **46**, pp. R1709-R1712 1992.
7. A. R. Bulsara, and G. Schneringer, "Stochastic resonance in globally coupled nonlinear oscillators," *Phys. Rev. E* **47**, pp. 3734-3737 1993.
8. J. F. Lindner, B. K. Meadows, and W. L. Ditto, "Array enhanced stochastic resonance and spatiotemporal synchronization," *Phys. Rev. Lett.* **75**, pp. 3-6 1995.
9. J. J. Collins, C. C. Chow, and T. T. Imhoff, "Stochastic resonance without tuning," *Nature* **376**, pp. 236-238 1995.
10. N. G. Stocks, "Suprathreshold stochastic resonance in multilevel threshold systems," *Phys. Rev. Lett.* **84**, pp. 2310-2313 2000.
11. P. Jung, and G. Mayer-Kress, "Spatiotemporal stochastic resonance in excitable media," *Phys. Rev. Lett.* **74**, pp. 2130-2133 1995.
12. M. F. Carusela, R. P. J. Perazzo, and L. Romanelli, "Stochastic resonant memory storage device," *Phys. Rev. E* **64**, art.no. 031101 2001.
13. S. K. Han, W. S. Kim, and H. Kook, "Temporal segmentation of the stochastic oscillator neural networks," *Phys. Rev. E* **58**, pp. 2325-2334 1998.
14. Y. Shim, H. Hong, and M. Y. Choi, "Noise-enhanced temporal association in neural networks," *Phys. Rev. E* **65**, art. no. 036114 2002.
15. D. R. Chialvo, G. A. Cecchi, and M. O. Magnasco, "Noise-enhanced memory in extended excitable systems," *Phys. Rev. E* **61**, pp. 5654-5657 2000.
16. S. H. Strogatz, "Exploring complex networks," *Nature* **410**, pp. 268-276 2001.
17. R. Albert, and A. L. Barabási, "Statistical mechanics of complex networks," *Rev. Mod. Phys.* **74**, pp. 47-97 2002.
18. D.J. Watts, and S.H. Strogatz, Collective dynamics of 'small-world' networks, *Nature (London)* **393**, pp. 440-442 (1998).
19. M. E. J. Newman, and D. J. Watts, "Scaling and percolation in the small-world network model," *Phys. Rev. E* **60**, pp. 7332-7342 1999.
20. N. Mathias, and V. Gopal, "Small worlds: How and why?" *Phys. Rev. E* **63**, art. no. 021117 2001.
21. A. D. Sánchez, J. M. López, and M.A. Rodríguez, "Nonequilibrium phase transition in directed small-world networks," *Phys. Rev. Lett.* **88**, art. no. 048701 2002.
22. M. Barahona, and L. M. Pecora, "Synchronization in small-world systems," *Phys. Rev. Lett.* **89**, art. no. 054101 2002.
23. L. F. Lago-Fernandez, R. Huerta, F. Corbacho, and J.A. Sigüenza, "Fast response and temporal coherent oscillations in small-world networks," *Phys. Rev. Lett.* **84**, pp. 2758-2761 2000.
24. J. Shao, T.H. Tsao, and R. Butera, "Bursting without slow kinetics: A role for a small world?" *Neural Computation* **18**, pp. 2029-2035 2006.
25. A. Herzog, K. Kube, B. Michaelis, A. D. de Lima, and T. Voigt, "Displaced strategies optimize connectivity in neocortical networks," *Neurocomputing* **70**, pp. 1121-1129 2007.
26. R. Manev, H. Manev, "The meaning of mammalian adult neurogenesis and the function of newly added neurons: the "small-world" network," *Medical Hypotheses* **64**, pp. 114-117 2005.
27. Z. Gao, B. Hu, and G. Hu, "Stochastic resonance of small-world networks," *Phys. Rev. E* **65**, art. no. 016209 2001.
28. D. He, G. Hu, M. Zhan, W. Ren, and Z. Gao, "Pattern formation of spiral waves in an inhomogeneous medium with small-world connections," *Phys. Rev. E* **65**, art. no. 055204(R) 2002.
29. X. Wang, Y. Lu, M. Jiang, and Q. Ouyang, "Attraction of spiral waves by localized inhomogeneities with small-world connections in excitable media," *Phys. Rev. E* **69**, art. no. 056223 2004.

30. H. Hong, B. J. Jim, and M. Y. Choi, "Stochastic resonance in the driven Ising model on small-world networks," *Phys. Rev. E* **66**, art. no. 011107 2002.
31. O. Kwon, H. H. Jo, and H. T. Moon, "Effect of spatially correlated noise on coherent resonance in a networks of excitable cells," *Phys. Rev. E* **72**, art. no. 066121 2005.
32. M. Perc, "Stochastic resonance on excitable small-world network via a pacemaker," *Phys. Rev. E* **76**, art. no. 066203 2007.
33. X. Sun, M. Perc, Q. Lu, and J. Kurths, "Spatial coherence resonance on diffusive and small-world networks of Hodgkin-Huxley neurons," *Chaos* **18**, art. no. 023102 2008.
34. Q. Li, and Y. Gao, "Control of spiking regularity in a noisy complex neural network," *Phys. Rev. E* **77**, art. no. 036117 2008.
35. F. Duan, F. Chapeau-Blondeau, and D. Abbott, "Stochastic resonance in a parallel array of nonlinear dynamical elements," *Phys. Lett. A* **372**, pp. 2159-2166 2008.
36. F. Duan, D. Rousseau, and F. Chapeau-Blondeau, "Residual aperiodic stochastic resonance in a bistable dynamic system transmitting a suprathreshold binary signal," *Phys. Rev. E* **69**, art. no. 011109 2004.